

Discrete Mechanics and Optimal Control Applied to the Compass Gait Biped

David Pekarek, Aaron D. Ames, and Jerrold E. Marsden

Abstract—This paper presents a methodology for generating locally optimal control policies for simple hybrid mechanical systems, and illustrates the method on the compass gait biped. Principles from discrete mechanics are utilized to generate optimal control policies as solutions of constrained nonlinear optimization problems. In the context of bipedal walking, this procedure provides a comparative measure of the suboptimality of existing control policies. Furthermore, our methodology can be used as a control design tool; to demonstrate this, we minimize the *specific cost of transport of periodic orbits for the compass gait biped, both in the fully actuated and underactuated case.*

I. INTRODUCTION

The compass gait biped is a two-dimensional bipedal robot that is simple enough to be amenable to analysis, yet complex enough to display a wealth of interesting phenomena. Most notably, this model exhibits stable passive gaits on a range of downhill slopes (see [4] and [8]). The work of Spong and Bullo [13] uses the technique of *controlled symmetries* to, with actuation, mimic passive gaits on level ground and uphill slopes. While this control strategy results in stable walking gaits, no formal assessment of its optimality has been made—this is a common phenomenon among control policies for bipedal walkers, and more generally simple hybrid mechanical systems (SHMS’s). This paper, therefore, has two objectives: assess the optimality of a given control strategy, and systematically construct optimal walking gaits.

One may evaluate the performance of the compass gait biped under controlled symmetries, or any other control policy, according to a variety of metrics: input norm, total energy usage, average speed, specific cost of transport, etc. To determine a given policy’s degree of suboptimality with respect to these metrics, we make use of Discrete Mechanics and Optimal Control (DMOC) [5], which efficiently provides locally optimal control policies for trajectories that have been discretized with respect to time based on principles from discrete mechanics. (Other optimization methods, not based on discrete mechanics have been implemented to produce controllers for bipedal walkers; for example, [3] and [10].)

Using DMOC to optimize the controlled trajectory between the boundary conditions—meaning states of the biped before and after impact with the ground—of a given control

policy yields a locally optimal cost functional for a given performance metric. This cost functional indicates the relative optimality or suboptimality of the given control policy.

The applications of DMOC to the compass biped extend beyond comparisons with existing control policies. Rather than deriving boundary conditions from an existing control law, they can be optimally chosen by way of a multi-layered optimization scheme. The fundamental idea underlying the scheme is to allow DMOC to optimize trajectories between given boundary conditions in an “inner-loop”, while a general non-linear optimization algorithm perturbs and optimizes the boundary conditions in an “outer-loop”. Solutions serve as limit cycle inducing control policies that are locally optimal with respect to both the continuous portion of the trajectory, and the impact conditions of the biped. That is, we *systematically obtain locally optimal walking gaits.*

The structure of this paper is as follows. Section II reviews the theory underlying simple hybrid mechanical systems, and the model of the compass biped in this framework. Section III presents the DMOC method of generating optimal controls, reviews controlled symmetries, and presents results in which DMOC has been used as a comparative tool. Section IV presents the two-layered optimization scheme, called “Simple Hybrid DMOC”, identifying the conditions necessary in applying it to an arbitrary SHMS. Section V presents the results obtained by applying Simple Hybrid DMOC to the compass biped.

II. SIMPLE HYBRID MECHANICAL SYSTEMS

Simple hybrid mechanical systems are a class of hybrid systems with continuous behavior in the form of Lagrangian dynamics. The compass biped and other walkers are naturally modeled by hybrid systems of this form; their continuous dynamics are obtained in the standard way via Lagrangian(s) and their discrete behavior is captured by impact equations describing the instantaneous change in the velocity of the system when the foot impacts the ground. This section, therefore, introduces the concepts of hybrid systems, Lagrangian dynamics, simple hybrid mechanical systems, hybrid flows, and hybrid periodic orbits.

Definition 1: A simple hybrid control system [2] is a tuple

$$\mathcal{HC} = (D, U, G, R, f, g),$$

where

- $D \subseteq \mathbb{R}^n$ is a smooth submanifold of \mathbb{R}^n , called the *domain*,
- $U \subseteq \mathbb{R}^k$ is a set of *admissible controls*,

D. Pekarek is with the Mechanical Engineering Department at the California Institute of Technology, Pasadena CA 91125 pekarek@caltech.edu

A. D. Ames and J. E. Marsden are with the Control and Dynamical Systems Department, California Institute of Technology, Pasadena, CA 91125 {ames, marsden}@cds.caltech.edu

- $G \subset D$ is subset of D called the *guard*,
- $R : G \rightarrow D$ is a smooth map called the *reset map*,
- (f, g) is a *control system*, i.e., $\dot{x} = f(x) + g(x)u$.

A *simple hybrid system*, \mathcal{H} , is a tuple $\mathcal{H} = (D, G, R, f)$, where f is a vector field on D , i.e., $\dot{x} = f(x)$.

Lagrangian Dynamics. As in [12], consider a mechanical system with a *configuration space*, Q , assumed to be a smooth manifold with a tangent bundle, TQ . The mechanical systems we will take into consideration have Lagrangians, $L : TQ \rightarrow \mathbb{R}$, given in coordinates by:

$$L(q, \dot{q}) = \frac{1}{2} \dot{q}^T M(q) \dot{q} - V(q),$$

where $M(q)$ is the inertial matrix, $\frac{1}{2} \dot{q}^T M(q) \dot{q}$ is the kinetic energy, and $V(q)$ is the potential energy. Applying Hamilton's Variational principle to these systems yields Euler-Lagrange equations of the form:

$$M(q)\ddot{q} + C(q, \dot{q})\dot{q} + N(q) = 0,$$

where $C(q, \dot{q})$ is commonly referred to as the Coriolis matrix and $N(q) = \frac{\partial V}{\partial q}(q)$. The vector field associated with these equations of motion has the form:

$$f_L(q, \dot{q}) = \begin{pmatrix} \dot{q} \\ M(q)^{-1}(-C(q, \dot{q})\dot{q} - N(q)) \end{pmatrix}. \quad (1)$$

In controlled cases, using the Lagrange-D'Alembert Principle will yield equations of motion of the form:

$$M(q)\ddot{q} + C(q, \dot{q})\dot{q} + N(q) = Bu,$$

where u is a vector of control inputs and B is a matrix mapping u to the system's generalized forces. These forced equations of motion lead to the control system (f_L, g_L) , where f_L is the vector field given in (1) and

$$g_L(q, \dot{q}) = \begin{pmatrix} 0_{n \times n} \\ M(q)^{-1}B \end{pmatrix}, \quad (2)$$

where $0_{n \times n}$ is an $n \times n$ matrix of zeros with $n = \dim(Q)$. Now we use these concepts regarding Lagrangian dynamics to formally define simple hybrid mechanical systems.

Definition 2: A *simple hybrid mechanical control system (SHMCS)* is a simple hybrid control system,

$$\mathcal{H}\mathcal{C}_L = (D, U, G, R, f_L, g_L),$$

where the control system (f_L, g_L) is the control system obtained from a Lagrangian L , as given in (1) and (2).

A *simple hybrid mechanical system (SHMS)* is a simple hybrid system $\mathcal{H}_L = (D, G, R, f_L)$ with f_L given as in (1).

Hybrid flows. A *hybrid flow* of a simple hybrid system \mathcal{H} is a tuple $\chi^{\mathcal{H}} = (\Lambda, \mathcal{J}, \mathcal{C})$, where

- $\Lambda = \{0, 1, 2, \dots\} \subseteq \mathbb{N}$ is an indexing set.
- $\mathcal{J} = \{I_i\}_{i \in \Lambda}$ is a *hybrid interval* where $I_i = [\tau_i, \tau_{i+1}]$ if $i, i+1 \in \Lambda$ and $I_{N-1} = [\tau_{N-1}, \tau_N]$ or $[\tau_{N-1}, \tau_N)$ or $[\tau_{N-1}, \infty)$ if $|\Lambda| = N$, N finite. Here, $\tau_i, \tau_{i+1}, \tau_N \in \mathbb{R}$ and $\tau_i \leq \tau_{i+1}$.
- $\mathcal{C} = \{c_i\}_{i \in \Lambda}$ is a collection of integral curves of f , i.e., $\dot{c}_i(t) = f(c_i(t))$ for all $i \in \Lambda$.

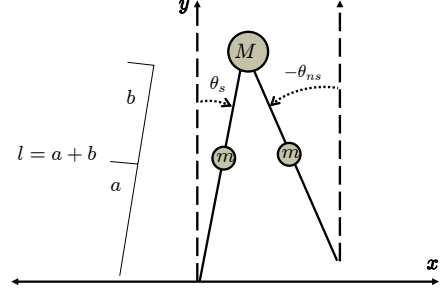


Fig. 1. The two-dimensional compass biped.

We require that the following conditions hold for every $i, i+1 \in \Lambda$,

- (i) $c_i(\tau_{i+1}) \in G$,
- (ii) $R(c_i(\tau_{i+1})) = c_{i+1}(\tau_{i+1})$.

The *initial condition* for the hybrid flow is $c_0(\tau_0)$. Note that we will assume “forced” semantics, meaning that $\tau_{i+1} = \min\{t \in \mathbb{R} : c_i(t) \in G\}$.

Hybrid periodic orbits. In the context of bipedal robots, we are interested in discussing walking gaits, which correspond to periodic orbits of the SHMS. A hybrid flow $\chi^{\mathcal{H}} = (\Lambda, \mathcal{J}, \mathcal{C})$ of \mathcal{H} is *periodic* if

- $\Lambda = \mathbb{N}$,
- $\lim_{i \rightarrow \infty} \tau_i = \infty$,
- $c_i(\tau_i) = c_{i+1}(\tau_{i+1})$ for all $i \in \Lambda$.

A *hybrid periodic orbit* $\mathcal{O} \subset D$ is a subset of D such that

$$\mathcal{O} = \bigcup_{i \in \mathbb{N}} \{c_i(t) : t \in I_i\}$$

for some periodic hybrid flow $\chi^{\mathcal{H}}$.

Biped Model. We now consider the two-dimensional compass biped walking on flat ground (see Figure 1), and its corresponding SHMCS model. The following is precisely the model used in [2]. We denote the hybrid control system describing the compass biped as:

$$\mathcal{H}\mathcal{C}_{2D} = (D_{2D}, U_{2D}, G_{2D}, R_{2D}, f_{2D}, g_{2D})$$

The configuration space¹ for the 2D biped is $Q_{2D} = \mathbb{R}^2$ with coordinates $\theta = (\theta_{ns}, \theta_s)^T$ where θ_{ns} is the angle of the non-stance leg from vertical and θ_s is the angle of the stance leg from vertical.

The domain and guard are constructed by utilizing the constraint that the non-stance (swing) foot is not allowed to pass through the ground, i.e., by utilizing the *unilateral constraint* function $H_{2D}(\theta) = \cos(\theta_s) - \cos(\theta_{ns})$. In particular,

¹Technically, the configuration space is given by $Q_{2D} = \mathbb{T}^2$, the two torus. The motivation for taking the configuration space to be \mathbb{R}^2 is that for the subset U of \mathbb{T}^2 containing the angular values of interest, there is a diffeomorphism sending this subset to a subset of \mathbb{R}^2 . Therefore, we simply view the angles as being elements of \mathbb{R}^2 ; this allows us to consider coordinates which we can view as being globally defined.

the domain D_{2D} is given by requiring that the height of the swing foot always be positive

$$D_{2D} = \left\{ \begin{pmatrix} \theta \\ \dot{\theta} \end{pmatrix} \in \mathbb{R}^4 : H_{2D}(\theta) \geq 0 \right\}.$$

We put no restrictions on the set of admissible controls except that they can only directly affect the angular acceleration. Therefore, $U_{2D} = \mathbb{R}^2$.

The guard G_{2D} is the subset of the domain corresponding to the set of configurations in which the height of the swing foot is zero and infinitesimally decreasing. That is,

$$G_{2D} = \left\{ \begin{pmatrix} \theta \\ \dot{\theta} \end{pmatrix} \in \mathbb{R}^4 : H_{2D}(\theta) = 0, \left(\frac{\partial H_{2D}(\theta)}{\partial \theta} \right)^T \dot{\theta} < 0 \right\}$$

which is the set of states at which the biped's swing foot impacts the ground, i.e., these are the impact conditions.

The reset map R_{2D} for $\mathcal{H}\mathcal{C}_{2D}$ is computed using the methods outlined in [1] and [11]. It is given by:

$$R_{2D}(\theta, \dot{\theta}) = \begin{pmatrix} S_{2D}\theta \\ P_{2D}(\theta)\dot{\theta} \end{pmatrix},$$

where S_{2D} and $P_{2D}(\theta)$ are given in Table I of [2]. This map models a perfectly plastic impact between the swing foot and the ground, and thus instantaneously changes the biped's momentum.

Finally, the dynamics for $\mathcal{H}\mathcal{C}_{2D}$ are obtained from the Euler-Lagrange equations in the standard way. Specifically, the Lagrangian describing this system is:

$$L_{2D}(\theta, \dot{\theta}) = \frac{1}{2} \dot{\theta}^T M_{2D}(\theta) \dot{\theta} - V_{2D}(\theta),$$

where $M_{2D}(\theta)$ is the inertial matrix and $V_{2D}(\theta)$ is the potential energy (these can be found in Table I of [2]). Using the controlled Euler-Lagrange equations, the dynamics for the walker are given by:

$$M_{2D}(\theta)\ddot{\theta} + C_{2D}(\theta, \dot{\theta})\dot{\theta} + N_{2D}(\theta) = B_{2D}u,$$

where $C_{2D}(\theta, \dot{\theta})$ is the coriolis matrix and $N_{2D} = \frac{\partial V_{2D}(\theta)}{\partial \theta}$. These equations yield the control system (f_{2D}, g_{2D}) as outlined in (1) and (2). This completes the task of modeling of the compass biped as a SHMCS.

III. DMOC AS AN OPTIMALITY MEASURE

Having introduced the hybrid model of the compass biped, we propose assessing the optimality of control policies with DMOC; this will provide accurate estimates of locally optimal values of cost functionals. This section, therefore, outlines DMOC as an optimization tool, reviews controlled symmetries as a method of producing stable walking gaits, and presents results in which DMOC is used to comparatively assess optimality in the use of controlled symmetries.

DMOC. In section II, it was noted that the equations of motion for a forced system with Lagrangian dynamics, such as a SHMS, follow from the *Lagrange-d'Alembert principle*.

The principle requires that

$$\delta \int_0^T L(q(t), \dot{q}(t)) dt + \int_0^T u(t) \cdot \delta q(t) dt = 0$$

for all variations δq with $\delta q(0) = \delta q(T) = 0$. The work in [5] sets up optimal control problems as constrained nonlinear optimization problems by utilizing a discretization of this variational principle. The method begins by discretizing the trajectory $q(t)$ in the same manner as in variational integrator theory [7]. That is, the state space TQ is replaced by $Q \times Q$ and a discrete path $q_d : \{0, h, 2h, \dots, Nh = T\} \rightarrow Q$, $N \in \mathbb{N}$, is defined such that $q_k = q_d(kh)$; this is considered an approximation to $q(kh)$. Similarly, the forcing² $u(t)$ is approximated by a discrete force $u_d : \{0, h, 2h, \dots, Nh = T\} \rightarrow T^*Q$ (with $u_k = u_d(kh)$). Based on this discretization, the action integral in the Lagrange-d'Alembert principle is approximated at each time slice $[kh, (k+1)h]$ as

$$\begin{aligned} L_d(q_k, q_{k+1}) &:= hL \left(\frac{q_{k+1} + q_k}{2}, \frac{q_{k+1} - q_k}{h} \right) \\ &\approx \int_{kh}^{(k+1)h} L(q(t), \dot{q}(t)) dt, \end{aligned}$$

where the midpoint rule was used to approximate $q(t)$ and $\dot{q}(t)$ on the slice as $(q_{k+1} + q_k)/2$ and $(q_{k+1} - q_k)/h$, respectively. Similarly, the virtual work expression in the principle is approximated at each slice as

$$\begin{aligned} u_k^- \cdot \delta q_k + u_k^+ \cdot \delta q_{k+1} &:= \frac{h}{4} (u_{k+1} + u_k) \cdot \delta q_k + \frac{h}{4} (u_{k+1} + u_k) \cdot \delta q_{k+1} \\ &\approx \int_{kh}^{(k+1)h} u(t) \cdot \delta q(t) dt, \end{aligned}$$

where u_k^- and u_k^+ are termed the *left* and *right discrete forces*, respectively. In discrete time they are both approximated as $\frac{h}{4}(u_{k+1} + u_k)$. Summing these approximations over the discrete path defines a discrete version of the Lagrange-d'Alembert principle,

$$\delta \sum_{k=0}^{N-1} L_d(q_k, q_{k+1}) + \sum_{k=0}^{N-1} u_k^- \cdot \delta q_k + u_k^+ \cdot \delta q_{k+1} = 0,$$

for all variations $\{\delta q_k\}_{k=0}^N$ with $\delta q_0 = \delta q_N = 0$. This is equivalent to the system of *forced discrete Euler-Lagrange equations*

$$D_2 L_d(q_{k-1}, q_k) + D_1 L_d(q_k, q_{k+1}) + u_{k-1}^+ + u_k^- = 0,$$

for all $k \in \{1, \dots, N-1\}$, where the notation D_i indicates differentiation with respect to the i^{th} argument. The continuous time boundary conditions, $(q(0), \dot{q}(0))$ and $(q(T), \dot{q}(T))$, are related to a discrete path via standard and discrete Legendre transforms, which produce continuous and discrete notions of the system's momentum. Setting these momenta equal, as well as $q_0 = q(0)$ and $q_N = q(T)$, yields the discrete boundary conditions

$$\begin{aligned} D_2 L(q(0), \dot{q}(0)) + D_1 L_d(q_0, q_1) + u_0^- &= 0, \\ -D_2 L(q(1), \dot{q}(1)) + D_1 L_d(q_{N-1}, q_N) + u_{N-1}^+ &= 0. \end{aligned}$$

²In this section, for the sake of simplicity, we will assume that the control inputs $u(t)$ are coincident with the system's generalized forces, that is, $B = I$

The final step is to note that the continuous time cost functional

$$J(q, u) = \int_0^T C(q(t), \dot{q}(t), u(t)) dt,$$

where C is a given performance metric, can be approximated at every time slice $[kh, (k+1)h]$ as

$$\begin{aligned} C_d(q_k, q_{k+1}, u_k, u_{k+1}) \\ &:= hC\left(\frac{q_{k+1} + q_k}{2}, \frac{q_{k+1} - q_k}{h}, \frac{u_{k+1} + u_k}{2}\right) \\ &\approx \int_{kh}^{(k+1)h} C(q, \dot{q}, u) dt. \end{aligned}$$

To summarize the DMOC method, optimal control policies may be searched for as the solution to the following nonlinear optimization problem with equality constraints:

$$\text{Minimize } J_d(q_d, u_d) = \sum_{k=0}^{N-1} C_d(q_k, q_{k+1}, u_k, u_{k+1})$$

with respect to u_d , subject to the constraints $q_0 = q(0)$, $q_N = q(1)$ and

$$\begin{aligned} D_2L(q(0), \dot{q}(0)) + D_1L_d(q_0, q_1) + u_0^- &= 0, \\ D_2L_d(q_{k-1}, q_k) + D_1L_d(q_k, q_{k+1}) + u_{k-1}^+ + u_k^- &= 0, \\ -D_2L(q(1), \dot{q}(1)) + D_1L_d(q_{N-1}, q_N) + u_{N-1}^+ &= 0, \end{aligned}$$

for all $k \in \{1, \dots, N-1\}$.

Controlled Symmetries. Controlled symmetries is a technique previously introduced in [13] that shapes the potential of bipedal robotic walkers to allow for stable walking gaits on flat ground based on stable walking gaits down a slope (which exist and have been well studied in [4] and [8]). The technique relies on “rotating the world” via a group action. That is, consider the group action $\Psi : \mathbb{S}^1 \times Q_{2D} \rightarrow Q_{2D}$ denoted by $\Psi_\gamma(\theta) := (\theta_{ns} - \gamma, \theta_s - \gamma)^T$, for $\gamma \in \mathbb{S}^1$. Using this, define the following feedback control law:

$$u = K_{2D}^\gamma(\theta) = B_{2D}^{-1} \frac{\partial}{\partial \theta} (V_{2D}(\theta) - V_{2D}(\Psi_\gamma(\theta))).$$

The main result of [13] is that there exists³ a γ such that applying $u = K_{2D}^\gamma(\theta)$ to $\mathcal{H}\mathcal{C}_{2D}$ yields a stable walking gait, i.e., an exponentially stable hybrid periodic orbit⁴.

Performance Comparison. We now examine the optimality of controlled symmetries using the performance metric $C(q, \dot{q}, u) = \|u\|^2$. Since controlled symmetries produces hybrid periodic orbits, the cost functional attributed to the trajectory for a single hybrid interval, say $I_0 = [\tau_0, \tau_1]$ on which the biped takes a single step, will be valid on any and every following hybrid interval. Using $l = 1$ m, $m = 5$ kg, $M = 10$ kg, and $\gamma = \pi/50$ radians, the controlled symmetries method produces a hybrid periodic orbit for the

³This γ is not unique, but we will pick one once and for all.

⁴This fact was not analytically verified, but rather verified by numerically computing the Poincaré map for this system and the corresponding eigenvalues.

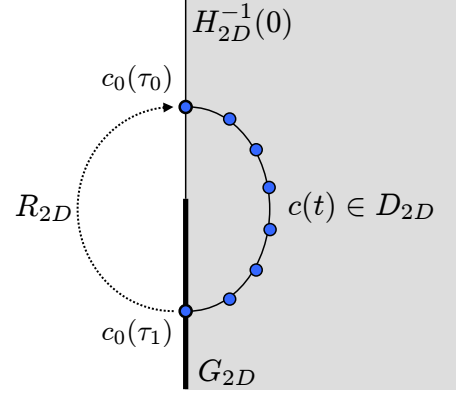


Fig. 2. The flow over one interval of a hybrid orbit of the compass biped. D_{2D} is bounded by the level set of the unilateral constraint function $H_{2D}^{-1}(0)$, which is indicated by the vertical line. G_{2D} is a subset of this boundary, represented in bold. The integral curve, $c(t)$, is dotted to indicate the discrete nature of our numerical simulations.

biped [2], which we’ll denote \mathcal{O}_{2D} . Simulation verifies that \mathcal{O}_{2D} intersects the guard at the following “impact” state:

$$\begin{pmatrix} \theta^* \\ \dot{\theta}^* \end{pmatrix} = \mathcal{O}_{2D} \cap G_{2D} \approx \begin{pmatrix} -0.2884 \\ 0.2884 \\ -1.6009 \\ -1.9762 \end{pmatrix}.$$

The initial state of the biped’s step is related to the impact state by the reset map R_{2D} . That is,

$$R_{2D}(\theta^*, \dot{\theta}^*) \approx \begin{pmatrix} 0.2884 \\ -0.2884 \\ -1.1235 \\ -0.2830 \end{pmatrix}.$$

The simulated flow connecting these initial and impact states is described graphically in Figure 2. The duration of I_0 in simulation is $(\tau_1 - \tau_0) \approx 0.7433$ s. Simulation provides a discrete approximation of the cost functional J , according to the same definition used in the DMOC. The discrete cost functional for this controlled symmetries step is $J_d = 8.0032$ Nms.

To provide an indication of the degree of optimality or sub-optimality in this controlled symmetries step we implement DMOC. The boundary conditions $q(0)$, $\dot{q}(0)$, $q(T)$, $\dot{q}(T)$ and T used for the method are provided by the controlled symmetries simulation. Specifically, we use $T = (\tau_1 - \tau_0)$, $(q(T), \dot{q}(T))^T = (\theta^*, \dot{\theta}^*)^T$, and $(q(0), \dot{q}(0))^T = R(\theta^*, \dot{\theta}^*)$. The DMOC optimization problem formulated using these boundary conditions is solved using sequential quadratic programming (SQP) methods, with the trajectory and controls from the controlled symmetries simulation serving as an initial guess. The solution to the optimization problem is a locally optimal discrete path, with an associated discrete cost functional of $J_d = 6.5192$ Nms. The results of the controlled symmetries simulation and DMOC optimization are presented in Figure 3. The similar phase portraits describing the two control laws indicate that while this implementation

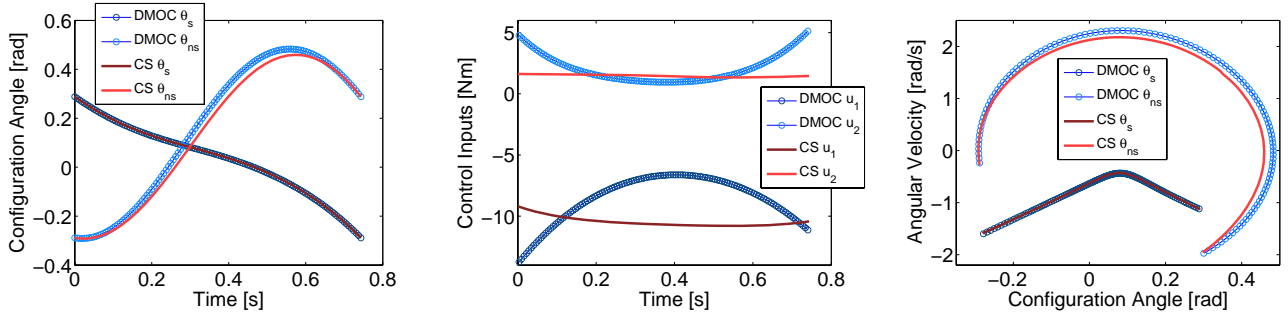


Fig. 3. A comparison of trajectories, inputs, and phase portraits for a single biped step controlled by the DMOC and Controlled Symmetries methods. Similarities in the phase portraits indicate that Controlled Symmetries is near a local optimum.

of controlled symmetries is suboptimal, it is near a locally optimal solution.

IV. SIMPLE HYBRID DMOC

In the previous section, DMOC was implemented as a comparison tool using boundary conditions from an existing control law in its implementation. DMOC may also be used as a control design tool for SHMS's, incorporated into a search for hybrid flows and limit cycles that are locally optimal in terms of both the discrete path on D and the conditions surrounding the resets at G . To accomplish this we present Simple Hybrid DMOC, a multi-layer optimization method akin to the decentralized method presented in [6].

The Inner Layer. The so-called “inner-layer” of Simple Hybrid DMOC performs the process completed in the previous performance comparison section. That is, given a set of boundary conditions $q(0)$, $\dot{q}(0)$, $q(T)$, $\dot{q}(T)$ and T , the DMOC optimization problem is formulated and solved using SQP methods. Denoting the set of discrete paths and controls obeying the DMOC constraints associated with the given set of boundary conditions as V , the solution to the optimization problem is a path \hat{q}_d and control \hat{u}_d such that $(\hat{q}_d, \hat{u}_d) \in V$ and $J_d(\hat{q}_d, \hat{u}_d)$ is a local optimum. Previously the controlled symmetries trajectory was used as an initial guess for the optimization. When implementing Simple Hybrid DMOC on systems where such a convenient initial guess is not available, one may substitute more heuristic approaches such as using linear trajectories connecting the boundary conditions.

The Outer Layer. The “outer-layer” of Simple Hybrid DMOC defines the inner layer's boundary conditions as optimization variables and attempts to minimize, as a function of these variables, the cost functional J_d for an entire hybrid flow. We first consider applying the method to a hybrid flow over a $N + 1$ hybrid intervals, meaning $\Lambda = \{0, 1, \dots, N\}$ where $N \in \mathbb{N}$ is finite. The method holds fixed the initial and final states of the hybrid flow, $c_0(\tau_0)$ and $c_N(\tau_{N+1})$, where the state $c(t)$ is shorthand for $(q(t)^T, \dot{q}(t)^T)^T$. The method varies the states corresponding to all other hybrid interval endpoints, denoted C_{bc} , as well as the lengths of all

the hybrid intervals, T_{bc} . These are defined as

$$C_{bc} = \{c_i(\tau_{i+1})\}_{i \in \Lambda \setminus N} \cup \{c_{i+1}(\tau_{i+1})\}_{i \in \Lambda \setminus N},$$

$$T_{bc} = \{(\tau_{i+1} - \tau_i)\}_{i \in \Lambda \setminus N},$$

respectively. These variables are constrained such that $c_i(\tau_{i+1}) \in G$ and $R(c_i(\tau_{i+1})) = c_{i+1}(\tau_{i+1})$, according to the definition of a hybrid flow. For all $i \in \Lambda$, we will use $q_{d,i}$ and $u_{d,i}$ to denote the path and control respectively on the hybrid interval I_i , and \tilde{J}_d to denote the discrete cost functional for a hybrid flow consisting only of locally optimal discrete paths. With these notations the optimization problem that the outer-loop solves has the form:

$$\text{Minimize } \tilde{J}_d(C_{bc}, T_{bc}) = \sum_{i=0}^N J_d(\hat{q}_{d,i}, \hat{u}_{d,i}),$$

subject to the constraints:

$$c_i(\tau_{i+1}) \in G$$

$$R(c_i(\tau_{i+1})) = c_{i+1}(\tau_{i+1})$$

for all $i \in \Lambda \setminus N$. The dependence of \tilde{J}_d on C_{bc} and T_{bc} comes in defining, for each interval I_i , the admissible set V_i to which $q_{d,i}$ and $u_{d,i}$ must belong.

The above optimization problem is easily adapted to the case of hybrid periodic orbits. In this case $N = 0$ since the optimization of boundary conditions for a single interval will extend to all other intervals. The concept of the fixed $c_0(\tau_0)$ and $c_N(\tau_{N+1})$ is removed, since the orbit's flow is not finite. The optimization variables are the boundary conditions for the single interval in consideration, that is $C_{bc} = \{c_0(0), c_0(\tau_1)\}$ and $T_{bc} = \{\tau_1\}$ where w.l.o.g. we have set $\tau_0 = 0$.

Solving the outer-loop optimization problem was also performed using SQP methods. Since one cost function evaluation in the outer loop requires solving one or more inner loop optimization problems, the Simple Hybrid DMOC method as it is currently constituted cannot be recommended for high dimensional hybrid systems. For the two-dimensional compass biped, however, the inner loop runs rapidly and thus the outer loop problem is computationally tractable.

Validity of Results. The constraints in the outer-loop optimization problem ensure that $c_i(\tau_{i+1}) \in G$, meaning

that each hybrid interval ends with system encountering the guard. However, it may be the case that there exists $t \in (\tau_i, \tau_{i+1})$ such that $c_i(t) \in G$, meaning that the solution intersects the guard prior to the end of a hybrid interval. Upon obtaining Simple Hybrid DMOC optimization results, they must be validated by checking that this condition is not present and thus no state resets have been ignored.

V. RESULTS FOR THE COMPASS GAIT BIPED

Attempts to implement Simple Hybrid DMOC on the compass biped using $C(q, \dot{q}, u) = \|u\|^2$ yielded the same trivial locally optimal discrete solution—a step of zero length in zero time. While it is true that no control is required for the biped to stand vertically, this is hardly an interesting result. Hence, we began using:

A New Performance Metric. Consider the metric termed the *specific cost of transport*, or *specific resistance* [9], defined for a cyclical gait as

$$\eta = \frac{P_{\text{avg}}}{W \cdot V_{\text{avg}}}$$

where P_{avg} is the average power dissipated over a step, W is the weight of the biped, and V_{avg} is the average velocity over a step. Noting that $P_{\text{avg}}/V_{\text{avg}}$ is equal to the quotient of the work done by the control torques and the step length, we see that setting $J = \eta$ is equivalent to choosing

$$C(\theta, \dot{\theta}, u) = \frac{\|\dot{\theta}^T B u\|_1}{W \cdot (\sin(\theta_s(\tau_0)) + \sin(\theta_{ns}(\tau_0)))}$$

where the numerator expresses the instantaneous power provided by the controls, and the constant denominator is the product of weight and step length.

Fully Actuated Results. The trajectories, inputs, phase portrait and graphical snapshots of a Simple Hybrid DMOC solution for the fully actuated compass biped are presented in Figures 4 and 5. This solution provides $\tilde{J}_d = 0.013$, the lowest value of all of the local minima discovered. The step taken by the biped is slower and shorter than that of the Controlled Symmetries solution. However the Simple Hybrid DMOC step is conservative in terms of the net work done by the controls, forcing the biped mostly in instances where the angular velocities in $\dot{\theta}$ are small in magnitude.

Underactuated Results. The trajectories, inputs, phase portrait and graphical snapshots of a Simple Hybrid DMOC solution for an underactuated compass biped are presented in Figures 6 and 7. In this case u_1 , the driving torque at the stance “foot”, is set to zero. For this trajectory, $\tilde{J}_d = 0.027$ was achieved, marking a loss of performance in comparison to the fully actuated case. The similar shape of the θ_s and θ_{ns} trajectories in the second half of the step indicate that the relative motion of the hip joint is nearly zero, and thus the energy spent by the control is also small in magnitude in that interval. Qualitatively, the underactuated biped rapidly forces the swing leg forward, and then “waits” for gravity to force the remainder of its step. The initial forcing of the swing leg is relatively large ($u_2(0) = 38.44$ Nm), but is within realizable limits.

VI. CONCLUSIONS AND FUTURE WORK

DMOC has been validated as a useful tool for SHMS’s, especially those of low dimension, by formulating optimal control generation as a constrained nonlinear optimization problem. Using the compass gait biped, we have demonstrated that solving DMOC optimization problems to assess optimality in the performance of an existing control policy, as well as solving Simple Hybrid DMOC optimization problems in order to design locally optimal hybrid orbits, provides valuable insights into possible control strategies.

The walking gaits generated by Simple Hybrid DMOC have not been assessed in terms of their stability; we would, therefore, like to find a method for incorporating the stability of a limit cycle into our methodology. Similarly, it would be of interest to study the cost of tracking them as a reference trajectory. Finally, the DMOC method can only guarantee local optimality, and in our simulations the compass gait biped displayed a multitude of local minima. Incorporating discrete mechanics into methods seeking the global optimum of a cost functional, or bounds on it, remains an open task.

VII. ACKNOWLEDGMENTS

The authors gratefully acknowledge James Martin for his discussions and resources regarding the implementation of the DMOC method, and Robert Gregg for his assistance in developing code for the bipedal walker. JEM was partially supported by AFOSR Contract FA9550-05-1-0343.

REFERENCES

- [1] A. D. Ames, R. D. Gregg, E. Wendel, and S. Sastry, “Towards the geometric reduction of controlled three-dimensional bipedal robotic walkers,” in *3rd Workshop on Lagrangian and Hamiltonian Methods for Nonlinear Control (LHMNL06)*, Nagoya, Japan, 2006.
- [2] A. D. Ames and R. D. Gregg, “Stably Extending Two-Dimensional Bipedal Walking to Three Dimensions,” in *26th American Control Conference*, New York, NY, 2007.
- [3] V. Duindam, “Port-Based Modeling and Control for Efficient Bipedal Walking Robots,” PhD Thesis, University of Twente, March, 2006.
- [4] A. Goswami, B. Thuilot, and B. Espiau, “Compass-like biped robot part I : Stability and bifurcation of passive gaits,” 1996, rapport de recherche de IINRIA.
- [5] O. Junge, J. E. Marsden, and S. Ober-Blobaum, “Discrete mechanics and optimal control,” in *16th IFAC Congress*, (Praha), 2005.
- [6] O. Junge, J. E. Marsden, and S. Ober-Blobaum, “Optimal Reconfiguration of Formation Flying Spacecraft a Decentralized Approach,” in *45th IEEE Conf. on Decision and Control*, 5210–5215, 2006.
- [7] J. E. Marsden and M. West, “Discrete mechanics and variational integrators,” *Acta Numerica*, vol. 10, pp. 357–514, 2001.
- [8] T. McGeer, “Passive dynamic walking,” *International Journal of Robotics Research*, vol. 9, no. 2, pp. 62–82, 1990.
- [9] T. McGeer, “Dynamics and control of bipedal locomotion,” *Journal of Theoretical Biology*, 163: 277–314, 1993.
- [10] K.D. Mombaur, H.G. Bock and R.W. Longman, “Stable, unstable and chaotic motions of bipedal walking robots without feedback,” in *2nd International Conference on Control Of Oscillations And Chaos*, IEEE, 282–285, 2000.
- [11] B. Morris and J. W. Grizzle, “A restricted Poincaré map for determining exponentially stable periodic orbits in systems with impulse effects: Application to bipedal robots,” in *44th Conference on Decision and Control*, Seville, Spain, 2005.
- [12] R. M. Murray, Z. Li, and S. Sastry, *A Mathematical Introduction to Robotic Manipulation*, CRC Press, 1993.
- [13] M. W. Spong and F. Bullo, “Controlled symmetries and passive walking,” *IEEE Transactions on Automatic Control*, vol. 50, no. 7, pp. 1025–1031, 2005.

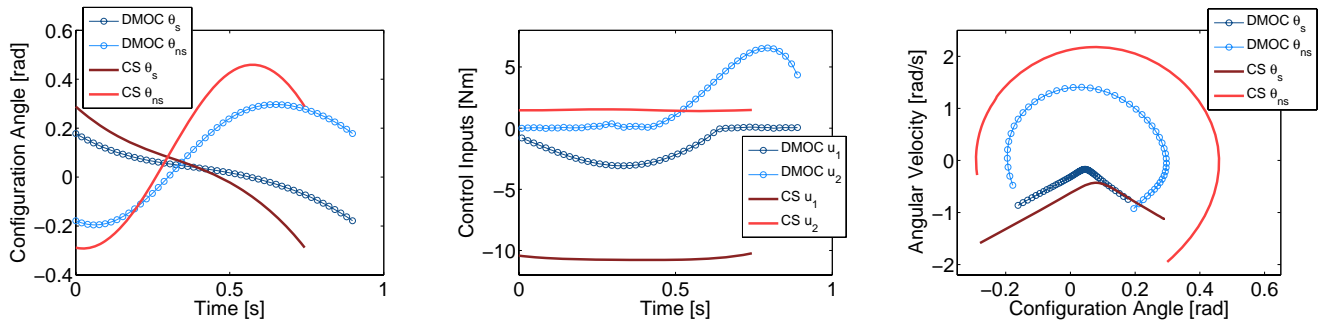


Fig. 4. A locally optimal Simple Hybrid DMOC solution. The previous Controlled Symmetries results are left in for reference.

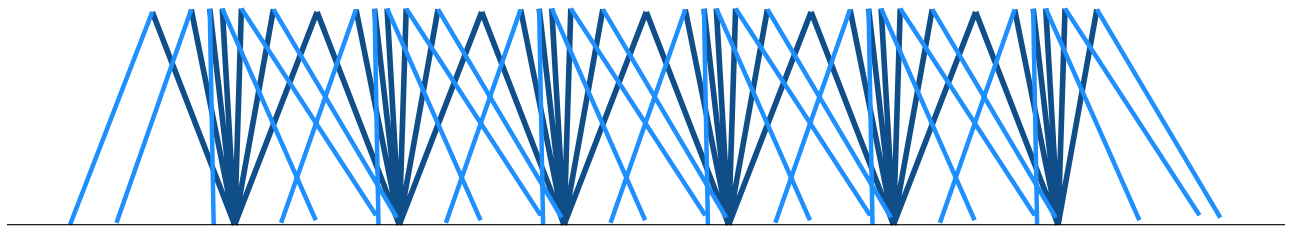


Fig. 5. Snapshots of the fully actuated simple hybrid DMOC solution at evenly spaced intervals of ≈ 0.18 s apart. The step length is not to scale for visualization purposes; in reality one step of the biped is equal to 35% of its height.

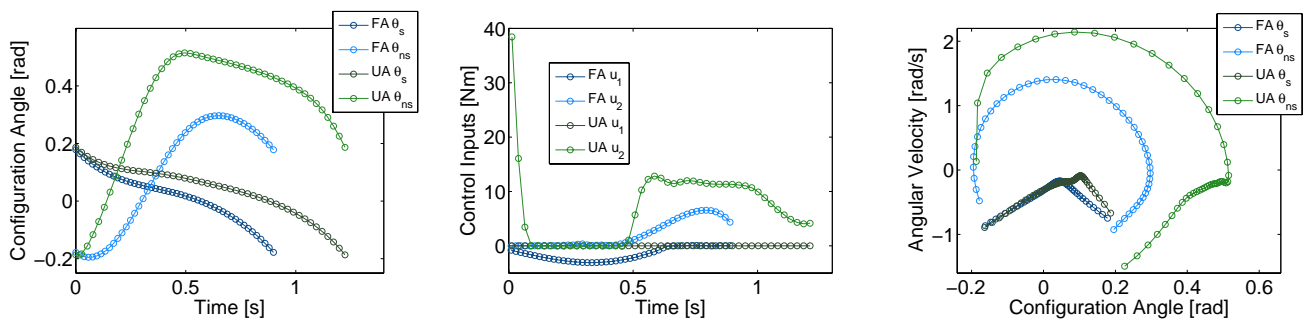


Fig. 6. Simple Hybrid DMOC solutions for both fully actuated (FA) and underactuated (UA) cases of the biped.

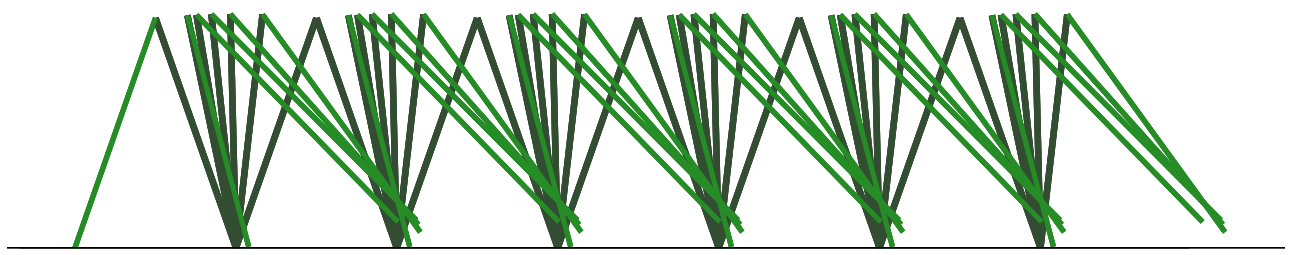


Fig. 7. Snapshots of the underactuated simple hybrid DMOC solution at evenly spaced intervals of ≈ 0.20 s apart. In reality one step of the biped is equal to 37% of its height.